Editors' Suggestion

Quantitative Assessment of the Toner and Tu Theory of Polar Flocks

Benoît Mahault,[1,2] Francesco Ginelli,[3,4] and Hugues Chaté[1,5,6]
[1]Service de Physique de l'Etat Condensé, CEA, CNRS, Université Paris-Saclay, CEA-Saclay, 91191 Gif-sur-Yvette, France
[2]Max Planck Institute for Dynamics and Self-Organization (MPIDS), 37077 Göttingen, Germany
[3]Department of Physics and Institute for Complex Systems and Mathematical Biology, Kings College, University of Aberdeen, Aberdeen AB24 3UE, United Kingdom
[4]Dipartimento di Scienza e Alta Tecnologia and Center for Nonlinear and Complex Systems, Università degli Studi dell'Insubria, Via Valleggio 11, 22100 Como, Italy
[5]Beijing Computational Science Research Center, Beijing 100094, China
[6]LPTMC, CNRS UMR 7600, Université Pierre et Marie Curie, 75252 Paris, France

(Received 5 September 2019; published 19 November 2019)

We present a quantitative assessment of the Toner and Tu theory describing the universal scaling of fluctuations in polar phases of dry active matter. Using large-scale simulations of the Vicsek model in two and three dimensions, we find the overall phenomenology and generic algebraic scaling predicted by Toner and Tu, but our data on density correlations reveal some qualitative discrepancies. The values of the associated scaling exponents we estimate differ significantly from those conjectured in 1995. In particular, we identify a large crossover scale beyond which flocks are only weakly anisotropic. We discuss the meaning and consequences of these results.

DOI: 10.1103/PhysRevLett.123.218001

Two seminal papers, both published in this journal in 1995, can be argued to mark the birth of active matter physics. In Ref. [1], Vicsek and collaborators introduced their simple model for collective motion, where XY spins fly at a constant speed along their magnetic direction. In Ref. [2], Toner and Tu (TT) wrote down fluctuating hydrodynamic equations for this flying XY model and performed a dynamic renormalization group calculation of its ordered phase, concluding, among other things, that such polar flocks possess true long-range orientational order even in two space dimensions (2D). In other words, flying spins defy the famous Mermin-Wagner theorem [3]. Since then, our knowledge of active matter has expanded tremendously (see, e.g., the various review papers [4–15]). But the TT papers remain influential even though they deal with the limit case of dilute, aligning, dry active matter, which usually consists of self-propelled particles subjected to local alignment in the absence of any surrounding fluid [15]. In particular, the TT theory (and related works by Ramaswamy *et al.*) predicted what has become one of the most popular features in active matter studies, the presence, in orientationally ordered phases, of "giant number fluctuations" (GNFs) where the variance of the number of particles in subsystems of increasing size scales faster than the mean [16–24].

Over the years, numerous numerical and experimental works have tried to verify the TT results, but the evidence presented has been restricted to a limited range of scales [25] and/or isotropic measures averaged over all spatial directions that cannot resolve individual scaling exponents [19,23,26], resulting in exponent values that could only be deemed compatible with the TT predictions. This situation was satisfactory as long as the TT theory was believed, as claimed in the early papers [2,27], to be "exact at all orders" in 2D, the dimension of choice of most works. However, Toner himself realized in 2012 [28] that this is not actually true and that a number of important terms have been overlooked, invalidating most claims of exactness. The remarkable result of true long-range order in 2D remains valid, as well as the overall structure of the theory. But, from then on, some features, and, in particular, the scaling exponent values, became predictions based on the hypothesis that the terms mentioned above are irrelevant. In spite of this situation, not much further numerical effort was devoted to gauge the accuracy of the TT predictions (see, however, Refs. [29,30]), and a full-fledged, quantitative evaluation of the TT theory is still missing.

In this Letter, we present large-scale numerical simulations of the Vicsek model designed to study the 2D and 3D anisotropic space-time correlations functions at the heart of the TT theory. Our results largely confirm its qualitative validity, but our estimates of exponent values clearly differ from the conjectured ones. In particular, we find that anisotropy is weak, possibly vanishing. Moreover, the behavior of density correlations shows qualitative discrepancies with the theory. We discuss their origin as well as the theoretical consequences of the hyperscaling relations that we find numerically satisfied.

We start with a synthetic account of the TT theory. The hydrodynamic equations written by Toner and Tu govern a conserved density ρ and a velocity field $\mathbf{v}$:

$$\partial_t \rho + \nabla \cdot (\rho \mathbf{v}) = 0, \tag{1a}$$

$$\partial_t \mathbf{v} + \lambda_1 (\mathbf{v}\cdot\nabla)\mathbf{v} + \lambda_2 (\nabla\cdot\mathbf{v})\mathbf{v} + \lambda_3 \nabla|\mathbf{v}|^2 = [\alpha - \beta|\mathbf{v}|^2]\mathbf{v} - \nabla P + D_0\nabla^2\mathbf{v} + D_1\nabla(\nabla\cdot\mathbf{v}) + D_2(\mathbf{v}\cdot\nabla)^2\mathbf{v} + \mathbf{f}. \tag{1b}$$

Here all coefficients can, in principle, depend on ρ and $|\mathbf{v}|$, the pressure P is expressed as a series in the density, and $\mathbf{f}$ is an additive noise with zero mean and variance Σ delta-correlated in space and time. To obtain the quantities of interest hereafter, i.e., correlation functions of density and transverse velocity fluctuations, Eq. (1) are linearized around the homogeneous ordered solution: $\rho = \rho_0 + \delta\rho$ and $\mathbf{v} = (v_0 + \delta v_\parallel)\hat{\mathbf{e}}_\parallel + \delta\mathbf{v}_\perp$, with ρ_0 the global density and $v_0 = \sqrt{\alpha/\beta}$. (Hereafter, subscripts $_\parallel$ and $_\perp$ refer, respectively, to directions longitudinal and transverse to the global order.) After enslaving the fast field $\delta v_\parallel$, the Fourier-transformed slow fluctuations read, in the small $q = |\mathbf{q}|$ limit [28],

$$\langle|\delta\rho(\omega,\mathbf{q})|^2\rangle = \frac{\rho_0^2\Sigma}{\mathcal{S}(\omega,\mathbf{q})} q_\perp^2, \tag{2a}$$

$$\langle|\delta\mathbf{v}_\perp(\omega,\mathbf{q})|^2\rangle = \frac{\Sigma(\omega - v_2 q_\parallel)^2}{\mathcal{S}(\omega,\mathbf{q})} + \frac{\Sigma(d-2)}{\mathcal{S}_T(\omega,\mathbf{q})}, \tag{2b}$$

where $\mathcal{S}(\omega,\mathbf{q}) = \{[\omega - c_+(\theta_\mathbf{q})q]^2 + \varepsilon_+^2(\mathbf{q})\}\{[\omega - c_-(\theta_\mathbf{q})q]^2 + \varepsilon_-^2(\mathbf{q})\}$, $\mathcal{S}_T(\omega,\mathbf{q}) = [\omega - c_T(\theta_\mathbf{q})q]^2 + \varepsilon_T^2(\mathbf{q})$, with $\theta_\mathbf{q}$ the angle between global order and $\mathbf{q}$, $q_\perp = |\mathbf{q}_\perp|$. The definitions of v_2, γ, $c_{\pm,T}(\theta_\mathbf{q})$, and $\varepsilon_{\pm,T}(\mathbf{q})$, which are unimportant for the following discussion, can be found in Ref. [28].

Equation (2a) implies the existence of propagative sound modes, or density waves, whose dispersion relations follow $\omega_\pm(\mathbf{q}) = c_\pm(\theta_\mathbf{q})q - \imath\varepsilon_\pm(\mathbf{q})$. This endows density fluctuations $\langle|\delta\rho(\omega,\mathbf{q})|^2\rangle$ with two sharp peaks in ω centered in $c_\pm(\theta_\mathbf{q})q$ and of respective widths $\varepsilon_\pm(\mathbf{q})$. The two terms of the rhs of Eq. (2b) correspond, respectively, to transverse velocity fluctuations parallel and perpendicular to $\mathbf{q}_\perp$. The first term represents correlations of $v_L = \delta\mathbf{v}_\perp\cdot\hat{\mathbf{q}}_\perp$, which behave like the density fluctuations. The second term denotes the fluctuations of $\mathbf{v}_T = \delta\mathbf{v}_\perp - v_L\hat{\mathbf{q}}_\perp$, which exist only for $d > 2$, and yields a third peak centered in $c_T(\theta_\mathbf{q})q$, of width $\varepsilon_T(\mathbf{q})$.

Since $\varepsilon_{\pm,T}(\mathbf{q})$ essentially scale as q^2 in the small wave number limit [28], the equal-time correlation functions are easily obtained by integrating Eq. (2) over ω. The resulting expressions, presented in Ref. [28], imply that $C_v(\mathbf{r}) = \langle\delta\mathbf{v}_\perp(\mathbf{0})\cdot\delta\mathbf{v}_\perp(\mathbf{r})\rangle \sim |\mathbf{r}|^{2-d}$ for $|\mathbf{r}|\to\infty$.

However, nonlinearities in Eq. (1) are relevant perturbations for all $d \le d_c = 4$ [28]. Equal-time velocity correlation functions in the nonlinear theory then follow $C_v(\mathbf{r}) \sim |\mathbf{r}|^\kappa$ for $|\mathbf{r}|\to\infty$, with $\kappa = 2\chi/\xi$ and 2χ, respectively, in the directions longitudinal and transverse to the order. The sound modes dampings are renormalized as well and read

$$\varepsilon(\mathbf{q}) \underset{q\to 0}{\sim} \{q_\perp^z \quad \text{for } q_\perp^\xi \gg q_\parallel; q_\parallel^{z/\xi} \quad \text{for } q_\parallel \gg q_\perp^\xi\}, \tag{3}$$

while the sound speeds $c_{\pm,T}(\theta_\mathbf{q})$ remain those given by the linear theory.

Exponents χ, ξ, and z are universal. The roughness exponent χ rules how the variance of velocity and density fluctuations varies with length scales. Fluctuations vanish asymptotically when $\chi < 0$, ensuring long-range polar order. The calculations of Toner and Tu proved that this is true for $d = 2$ and 3, while in the linear theory, where $\chi = 1 - d/2$, fluctuations diverge and order is destroyed in 2D. The anisotropy exponent ξ measures the difference in scaling along and transversally to global order. The TT theory predicts that fluctuations scale anisotropically for $d < d_c = 4$ ($\xi < 1$), while in mean field $\xi = 1$. Finally, the dynamical exponent z measures how the lifetime of sound modes scales with the system size. At the linear level $z = 2$, which corresponds to a diffusive damping, while $z < 2$ is expected for $d < 4$ according to the TT theory. In their first publications [2,27], Toner and Tu claimed an exact computation of these exponents in $d = 2$ and found $\chi = (3 - 2d)/5$ and $\xi = z/2 = (d+1)/5$ (see TT95 numbers in Table I). In his later "reanalysis" of the theory [28], Toner realized that additional relevant nonlinearities were missed, so that the above exponent values could be exact, even in $d = 2$, only under the conjecture of the asymptotic irrelevance of these terms.

We now turn to our numerical assessment of the TT theory. We use the standard discrete-time Vicsek model for efficiency. Particles $i = 1,\ldots,N$ with position $\mathbf{r}_i$ and orientation $\hat{\mathbf{e}}_i$ move at constant speed v_0 and align their velocities with current neighbors j:

$$\hat{\mathbf{e}}_i^{t+1} = \vartheta[\langle\hat{\mathbf{e}}_j^t\rangle_{j\sim i} + \eta\xi_i^t], \qquad \mathbf{r}_i^{t+1} = \mathbf{r}_i^t + v_0\hat{\mathbf{e}}_i^{t+1}, \tag{4}$$

where $\vartheta[\mathbf{u}] = \mathbf{u}/|\mathbf{u}|$, $\langle\rangle_{j\sim i}$ is the average over all particles j within unit distance of i (including i), and ξ_i^t are uncorrelated random vectors uniformly distributed on the unit

TABLE I. Exponent values conjectured by Toner and Tu in Ref. [2] and those resulting from our numerical evaluation of the density and velocity correlation functions.

	$d=2$		$d=3$		$d\ge 4$
	TT95	Numerics	TT95	Numerics	Mean-field
χ	−0.20	−0.31(2)	−0.60	$\simeq -0.62$	$1-d/2$
ξ	0.60	0.95(2)	0.80	$\simeq 1$	1
$\zeta \equiv d-1+2\chi+\xi$	1.20	1.33(2)	1.60	1.77(3)	2
z	1.20	1.33(2)	1.60	$\simeq 1.77$	2
GNFs	1.60	1.67(2)	1.53	1.59(3)	$1+2/d$

circle (2D) or sphere (3D) [31]. Square domains of linear size L containing $N = \rho_0 L^d$ particles, with N ranging from a few million to a few billion, were considered. For numerical efficiency, small speed and weak noise were avoided. We used $v_0 = 1$ and $\eta = 0.5$ (2D) and 0.45 (3D) with $\rho_0 = 2$, parameter values in the homogeneous ordered phase but not too deep inside. Fluctuation fields $\delta\rho$ and $\delta\mathbf{v}_\perp$ were obtained by coarse-graining over boxes of unit linear length. The associated correlation functions were simply obtained by computing the square norm of the fields' Fourier transform.

In finite systems with periodic boundary conditions, the direction of order diffuses slowly (the diffusion constant $\propto 1/N$ [39]). To estimate quantities scaling anisotropically like those defined by Eq. (2), one then needs, before averaging in time, to rotate a copy of the system at each measure so that the global order remains along a chosen direction. Moreover, data have then to be averaged over times longer than the timescale of this rotation. This is possible but costly and quickly becomes prohibitive for large systems. Forcing the global order to remain along a given direction can be achieved either by applying an external field or by imposing reflecting side boundaries as in, e.g., Refs. [25,29,30]. This perturbs slightly the global behavior of the system but allows for much shorter averaging times at equivalent sizes. All three protocols were tested, and we found that when used cautiously they yield identical results over the scales that can be explored by all (see [33] for details). Below, we present only data obtained using a channel with reflective walls.

Because the scaling of correlations in real space generally suffers strong finite-size effects [39], this work focuses on their analysis in Fourier space. Although we measured correlations in the whole $(q_\parallel, q_\perp)$ plane [40], exponents χ and ξ can be estimated from just the longitudinal ($q_\perp = 0$) and transverse ($q_\parallel = 0$) directions. For velocity correlations, we have

$$\langle|\delta\mathbf{v}_\perp(\mathbf{q})|^2\rangle \underset{q\to 0}{\sim} \{q_\perp^{-\zeta} \quad \text{for } q_\perp^{\xi} \gg q_\parallel; q_\parallel^{-\zeta/\xi} \quad \text{for } q_\parallel \gg q_\perp^{\xi}\} \tag{5}$$

with $\zeta \equiv d - 1 + 2\chi + \xi$. Our data in both 2D and 3D show that $\langle|\delta\mathbf{v}_\perp(\mathbf{q})|^2\rangle$ scales cleanly at small values of $q_\perp$ [lower sets of curves in Figs. 1(a) and 1(b)], with estimated values of ζ slightly but significantly different than those conjectured by Toner and Tu (see Table I). Behavior in the longitudinal direction is more surprising [upper set of curves in Figs. 1(a) and 1(b)]. While from Ref. [27] a divergence for $q_\parallel \to 0$ with an exponent -2 is conjectured in both 2D and 3D, we observe, in 2D, a *size-independent crossover* from a power law with exponent $\simeq -1.65$ at intermediate values of $q_\parallel$ to one with a *larger* exponent $\simeq -1.4$ at smaller $q_\parallel$. The crossover scale $\ell_c = 2\pi/q_c \simeq 100$, indicated by the purple dashed lines in our figures, is of the same order as typical sizes considered so far in other works [19,25], which may explain why it has never been reported. Note further that our postcrossover estimate -1.4 is not far from the -1.33 value measured in the transverse direction, implying weak, possibly vanishing, anisotropy ($\xi \simeq 0.95$). In 3D, the two correlation functions show approximately the same exponent above a scale $\ell_c \simeq 30$: Scaling is isotropic [Fig. 1(b)]. Overall, our measures lead to values of χ and ξ in clear departure from those conjectured by Toner and Tu (see Table I).

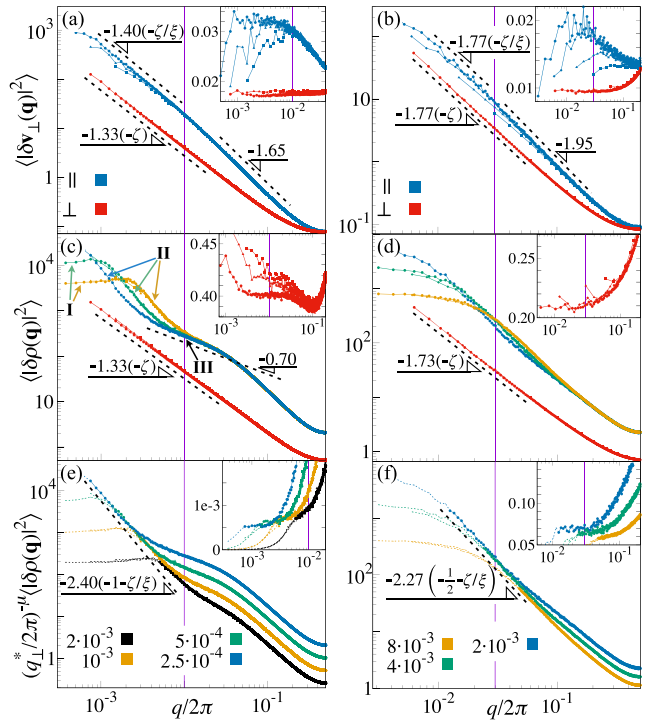

FIG. 1. Equal-time correlations in 2D (left) and 3D (right). Insets contain the same data as their main panel but rescaled by $(q/2\pi)^\sigma$, where σ is an estimated exponent. The purple vertical lines mark the crossover scale $q_c/(2\pi)$ (see the text). Symbol code for linear system size: in 2D, squares, triangles, and dots for $L = 2000$, 4000, and 8000, respectively; in 3D, squares, triangles, diamonds, and dots for $L = 100$, 200, 500, and 960, respectively. (a),(b) Velocity correlations in the transverse (red, lower data) and longitudinal (blue, upper data) directions. Insets: $\sigma = 1.33$ (2D, $\perp$), 1.40 (2D, $\parallel$), and 1.77 (3D, $\perp$ and $\parallel$). (c),(d) Density correlations in the transverse (red, lower data) and longitudinal directions for different values of $q_\perp^*$ (upper curves, shifted upward for clarity). In (c), Roman numerals indicate the three longitudinal scaling regimes discussed in the text (upper curves). Insets: $\sigma = 1.33$ (2D, $\perp$) and 1.73 (3D, $\perp$). (e),(f): Longitudinal data of (c),(d) rescaled by $q_\perp^{*\,-\mu}$ with $\mu = 1$ and $\frac{1}{2}$ in 2D and 3D, respectively. Points in the regime $q_\perp \gg q_\parallel$ are shown in thin dashed lines for clarity. Insets: $\sigma = 2.40$ (2D) and 2.27 (3D).

The density correlation function is expected to show the following longitudinal and transverse scalings [41]:

$$\langle|\delta\rho(\mathbf{q})|^2\rangle \underset{q\to 0}{\sim} \{q_\perp^{-\zeta} \quad \text{for } q_\perp \gg q_\parallel; q_\perp^2 q_\parallel^{-2-\zeta/\xi} \quad \text{for } q_\parallel \gg q_\perp^\xi\}. \tag{6}$$

In the transverse direction, our data confirm that scaling takes place with the same exponent as for velocity correlations [Figs. 1(c) and 1(d), lower set of curves], albeit with more pronounced finite-size effects, especially in 2D [compare the insets in Figs. 1(a) and 1(b) and Figs. 1(c) and 1(d); see [33] for comments]. In 3D, the apparent exponent is slightly lower in absolute value than the one given by $\langle|\delta\mathbf{v}_\perp(\mathbf{q})|^2\rangle$ (-1.73 vs -1.77), but given the limited range of scaling available we cannot exclude that these two values are, in fact, the same asymptotically.

The scaling of density fluctuations in the longitudinal direction is more subtle to analyze, because it depends explicitly on $q_\perp$ [see Eq. (6)]. The behavior of $\langle|\delta\rho(\mathbf{q})|^2\rangle$ with $q_\parallel$ for three fixed values of $q_\perp^*$ is shown in Figs. 1(c) and 1(d) (upper sets of curves). One can identify three regimes below the crossover scale $q_c = 2\pi/\ell_c$ [noted I, II, and III in Fig. 1(c)], which are most easily distinguished in 2D but probably also present in 3D. For the smallest values of $q_\parallel$, the functions reach a plateau, whose range of existence and amplitude, respectively, increases and decreases with $q_\perp^*$ (regime I). This behavior corresponds to the "transverse" regime where $q_\parallel \ll q_\perp$. Increasing $q_\parallel$ beyond this plateau, $\langle|\delta\rho(\mathbf{q})|^2\rangle$ shows a second scaling behavior with a $q_\perp^*$-dependent amplitude (regime II), in qualitative agreement with Eq. (6). Finally, in 2D, where sufficiently large systems can be studied, a third scaling region (regime III) is observed, with a slow (exponent ~ -0.7), $q_\perp^*$-independent decay whose range increases when $q_\perp^* \to 0$. Such a regime is absent from the framework of the TT theory.

The second regime also departs strikingly from the Toner-Tu results. In this region, both 2D and 3D curves do not collapse when their amplitude is rescaled by $q_\perp^{*-\mu}$ with $\mu = 2$, as predicted exactly by the TT theory, but rather with $\mu \simeq 1$ in 2D and 0.5 in 3D [Figs. 1(e) and 1(f)]. Moreover, the collapsed curves do not decay with exponent $-2-\zeta/\xi \simeq -3.4$ (2D) and $\simeq -3.77$ (3D) as predicted by Eq. (6) using the values of χ and ξ determined from $\langle|\delta\mathbf{v}_\perp(\mathbf{q})|^2\rangle$. Rather, we find -2.4 in 2D and -2.27 in 3D. Our data therefore suggest that, for $q_\parallel \gg q_\perp^\xi$, $\langle|\delta\rho(\mathbf{q})|^2\rangle \sim q_\perp^\mu q_\parallel^{-\mu-\zeta/\xi}$ with $\mu \simeq 1$ in 2D and 0.5 in 3D.

In order to assess the dynamical exponent z, we now turn to the study of space-time correlations. As expected from Eq. (2) and previous work in 2D [25,30], both $\langle|\delta\rho(\omega,\mathbf{q})|^2\rangle$ and $\langle|\delta\mathbf{v}_\perp(\omega,\mathbf{q})|^2\rangle$, as functions of ω, show two asymmetric peaks that become symmetric in the transverse direction ($\theta_\mathbf{q} = \pi/2$). In 3D, one observes the emergence of an additional third peak in $\langle|\delta\mathbf{v}_\perp(\omega,\mathbf{q})|^2\rangle$ coming from its component $\mathbf{v}_T$. All these peaks are well fitted close to their maximum by Cauchy distributions of the type $H_{\pm,T}(\mathbf{q})/\{1+[\omega-\omega^*_{\pm,T}(\mathbf{q})]^2/\Delta\omega^2_{\pm,T}(\mathbf{q})\}$, where $H_{\pm,T}(\mathbf{q})$, $\omega^*_{\pm,T}(\mathbf{q})$, and $\Delta\omega_{\pm,T}(\mathbf{q})$, respectively, account for their heights, positions, and half-peak widths (see data in Ref. [33]). Since we have seen that density correlations seem more sensitive to finite-size effects, we now focus on velocity correlations for the quantitative characterization of the peaks. As expected, peak positions $\omega^*_{\pm,T}(\mathbf{q})$ scale linearly with q in the limit $q \to 0$, and the sound speeds $c_{\pm,T}(\theta_\mathbf{q})$ are given by the corresponding slopes. Perfect agreement is found with the linear theory, in both 2D and 3D [39]. Peak widths, on the other hand, show nontrivial scaling: $\Delta\omega_{\pm,T}(\mathbf{q})$ correspond to the dampings $\varepsilon_{\pm,T}(\mathbf{q})$ and, thus, from Eq. (3) are expected to scale as $q_\parallel^{z/\xi}$ and $q_\perp^z$ in the longitudinal and transverse directions. We find rather good scaling in 2D for both longitudinal and transverse directions [Fig. 2(a)], with, in this last case, $z \simeq 1.33$. In the longitudinal direction, we find weak evidence of a crossover at the same scale ℓ_c as for equal-time correlations. Below ℓ_c, the estimated value of z/ξ (1.65) is identical to that of ζ/ξ found below ℓ_c in Fig. 1(a). Beyond ℓ_c, we unfortunately could not obtain much data, but the few points we have are compatible with a slope 1.4, i.e., the asymptotic value of ζ/ξ found from Fig. 1(a). In 3D, where the data are much more limited, we can nevertheless observe good scaling of the peak width $\Delta\omega_T(\mathbf{q})$ over almost a decade in the transverse direction $\theta_\mathbf{q} = \pi/2$, yielding the estimate $z \simeq 1.77$ [see Fig. 2(b)], identical to our estimate of ζ from equal-time correlations. Results leading to similar values of z in 2D and 3D are found from the scaling of the peaks heights; see [33] for details.

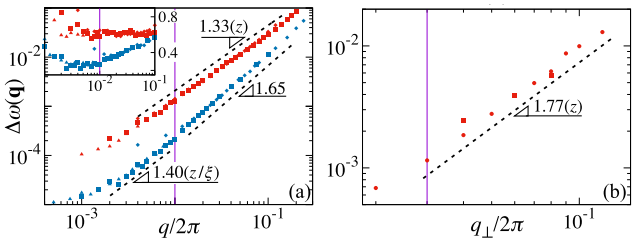

FIG. 2. (a) 2D peak widths as functions of q in the transverse (red, upper curves) and longitudinal (blue, lower curves) directions; insets: the same data rescaled by $(q/2\pi)^\sigma$ with, respectively, $\sigma = 1.33$ and 1.40. (Diamonds, squares, and triangles, respectively, correspond to system sizes $L = 1000$, 2000, and 4000.) (b) The same as (a) but in 3D and only in the transverse direction for the peak related to $\mathbf{v}_T$ (see [33]) at sizes $L = 100$ (squares) and 200 (dots).

In summary, using the Vicsek model, we have tested the structure and the quantitative predictions of the TT theory. While we find overall qualitative agreement with these remarkable results, our estimates of the three universal exponents χ, ξ, and z, which we have measured *independently*, are incompatible with those conjectured by Toner and Tu in Ref. [2] (see Table I). These differences indicate that

at least some of the nonlinearities identified in Ref. [28] and neglected in the original calculation are indeed relevant asymptotically.

Our data suggest, in particular, the existence of a crossover scale beyond which—i.e., at scales scarcely explored before—there is very little or vanishing anisotropy. Coming back to the popular giant number fluctuations, we find that ζ/d, which governs their scaling, varies very little across scales and takes values close to those predicted by Toner and Tu (see Table I and Ref. [33]). This clarifies why previous studies focusing on this quantity could not challenge the Toner and Tu conjecture [19,25,26].

We find identical estimates, within our numerical accuracy, of ζ and z. In other words, the hyperscaling relation $z = d - 1 + 2\chi + \xi$ seems satisfied. If we take this numerical fact for granted, it implies that, somewhat counterintuitively, the vertices responsible for the departure from the 1995 TT results are *not* those coupling density and order. Moreover, $\zeta = z$ also implies that the noise variance Σ does not renormalize, so that the dominant effective noise in the $\mathbf{v}$ equation is indeed additive, as assumed in the TT theory (see [33] for the simple arguments leading to these conclusions).

We also find qualitative discrepancies with the TT theory in the longitudinal behavior of density correlations [42]. We have at present no full understanding of this, but, as explained in a forthcoming publication, the consideration of a (conserved) additive noise in the density equation—something quite natural in the context of fluctuating hydrodynamic equations—leads to a modified form of Eq. (6) in the $q_\perp \to 0$ sector, while velocity fluctuations [Eq. (5)] remain unchanged. This change already occurs at the linear level and could account, upon renormalization, for the peculiar scaling regimes reported in Figs. 1(c)–1(f).

In spite of the above remarks, we believe our results bring further evidence that the TT theory is the correct framework to describe the universal properties of dry polar flocks. Nevertheless, we are still missing a final answer, and our findings call even more than before for a complete, possibly nonperturbative, renormalization group approach [43].

We thank Cesare Nardini and Aurelio Patelli for fruitful discussions. We acknowledge a generous allocation of CPU time on Beijing CSRC's Tianhe supercomputer.

[1] T. Vicsek, A. Czirók, E. Ben-Jacob, I. Cohen, and O. Shochet, Novel Type of Phase Transition in a System of Self-Driven Particles, Phys. Rev. Lett. **75**, 1226 (1995).

[2] J. Toner and Y. Tu, Long-Range Order in a Two-Dimensional Dynamical XY Model: How Birds Fly Together, Phys. Rev. Lett. **75**, 4326 (1995).

[3] N. D. Mermin and H. Wagner, Absence of Ferromagnetism or Antiferromagnetism in One- or Two-Dimensional Isotropic Heisenberg Models, Phys. Rev. Lett. **17**, 1133 (1966).

[4] Special Issue on Hydrodynamics and phases of flocks, edited by J. Toner, Y. Tu, and S. Ramaswamy [Ann. Phys. (Amsterdam) **318**, 170 (2005)].

[5] S. Ramaswamy, The mechanics and statistics of active matter, Annu. Rev. Condens. Matter Phys. **1**, 323 (2010).

[6] P. Romanczuk, M. Bär, W. Ebeling, B. Lindner, and L. Schimansky-Geier, Active Brownian particles, Eur. Phys. J. Spec. Top. **202**, 1 (2012).

[7] T. Vicsek and A. Zafeiris, Collective motion, Phys. Rep. **517**, 71 (2012).

[8] M. C. Marchetti, J. F. Joanny, S. Ramaswamy, T. B. Liverpool, J. Prost, M. Rao, and R. A. Simha, Hydrodynamics of soft active matter, Rev. Mod. Phys. **85**, 1143 (2013).

[9] M. E. Cates and J. Tailleur, Motility-induced phase separation, Annu. Rev. Condens. Matter Phys. **6**, 219 (2015).

[10] J. Elgeti, R. G. Winkler, and G. Gompper, Physics of microswimmers—Single particle motion and collective behavior: A review, Rep. Prog. Phys. **78**, 056601 (2015).

[11] J. Prost, F. Jülicher, and J.-F. Joanny, Active gel physics, Nat. Phys. **11**, 111 (2015).

[12] C. Bechinger, R. Di Leonardo, H. Löwen, C. Reichhardt, G. Volpe, and G. Volpe, Active particles in complex and crowded environments, Rev. Mod. Phys. **88**, 045006 (2016).

[13] S. Ramaswamy, Active matter, J. Stat. Mech. (2017) 054002.

[14] A. Doostmohammadi, J. Ignés-Mullol, J. M. Yeomans, and F. Sagués, Active nematics, Nat. Commun. **9**, 3246 (2018).

[15] H. Chaté, Dilute aligning dry active matter, Annu. Rev. Condens. Matter Phys. (to be published).

[16] S. Ramaswamy, R. A. Simha, and J. Toner, Active nematics on a substrate: Giant number fluctuations and long-time tails, Europhys. Lett. **62**, 196 (2003).

[17] H. Chaté, F. Ginelli, and R. Montagne, Simple Model for Active Nematics: Quasi-Long-Range Order and Giant Fluctuations, Phys. Rev. Lett. **96**, 180602 (2006).

[18] V. Narayan, S. Ramaswamy, and N. Menon, Long-lived giant number fluctuations in a swarming granular nematic, Science **317**, 105 (2007).

[19] H. Chaté, F. Ginelli, G. Grégoire, and F. Raynaud, Collective motion of self-propelled particles interacting without cohesion, Phys. Rev. E **77**, 046113 (2008).

[20] F. Ginelli, F. Peruani, M. Bär, and H. Chaté, Large-Scale Collective Properties of Self-Propelled Rods, Phys. Rev. Lett. **104**, 184502 (2010).

[21] H. P. Zhang, A. Be'er, E.-L. Florin, and H. L. Swinney, Collective motion and density fluctuations in bacterial colonies, Proc. Natl. Acad. Sci. U.S.A. **107**, 13626 (2010).

[22] S. Ngo, A. Peshkov, I. S. Aranson, E. Bertin, F. Ginelli, and H. Chaté, Large-Scale Chaos and Fluctuations in Active Nematics, Phys. Rev. Lett. **113**, 038302 (2014).

[23] F. Giavazzi, C. Malinverno, S. Corallino, F. Ginelli, G. Scita, and R. Cerbino, Giant fluctuations and structural effects in a flocking epithelium, J. Phys. D **50**, 384003 (2017).

[24] D. Nishiguchi, K. H. Nagai, H. Chaté, and M. Sano, Long-range nematic order and anomalous fluctuations in suspensions of swimming filamentous bacteria, Phys. Rev. E **95**, 020601(R) (2017).

[25] Y. Tu, J. Toner, and M. Ulm, Sound Waves and the Absence of Galilean Invariance in Flocks, Phys. Rev. Lett. **80**, 4819 (1998).
[26] H. Chaté, F. Ginelli, G. Grégoire, F. Peruani, and F. Raynaud, Modeling collective motion: Variations on the Vicsek model, Eur. Phys. J. B **64**, 451 (2008).
[27] J. Toner and Y. Tu, Flocks, herds, and schools: A quantitative theory of flocking, Phys. Rev. E **58**, 4828 (1998).
[28] J. Toner, Reanalysis of the hydrodynamic theory of fluid, polar-ordered flocks, Phys. Rev. E **86**, 031918 (2012).
[29] N. Kyriakopoulos, F. Ginelli, and J. Toner, Leading birds by their beaks: The response of flocks to external perturbations, New J. Phys. **18**, 073039 (2016).
[30] D. Geyer, A. Morin, and D. Bartolo, Sounds and hydrodynamics of polar active fluids, Nat. Mater. **17**, 789 (2018).
[31] Here we use this "vectorial noise" version, shown in Ref. [32] to be less sensitive to finite-size effects in the coexistence phase. We also used the more common "angular noise" version, obtaining similar results; see Ref. [33].
[32] G. Grégoire and H. Chaté, Onset of Collective and Cohesive Motion, Phys. Rev. Lett. **92**, 025702 (2004).
[33] See Supplemental Material at http://link.aps.org/supplemental/10.1103/PhysRevLett.123.218001 for details about numerical methods and measurement protocols, a discussion of GNFs scaling, additional information about space-time correlation functions, and comments on hyperscaling relations, which includes Refs. [34–38].
[34] H. H. Wensink and H. Löwen, Aggregation of self-propelled colloidal rods near confining walls, Phys. Rev. E **78**, 031409 (2008).
[35] F. Ginelli, The physics of the Vicsek model, Eur. Phys. J. Spec. Top. **225**, 2099 (2016).
[36] S. Ngo, Physique Statistique des Groupes en Mouvement, Ph.D. thesis, Université Pierre et Marie Curie, 2013.
[37] F. D. C. Farrell, M. C. Marchetti, D. Marenduzzo, and J. Tailleur, Pattern Formation in Self-Propelled Particles with Density-Dependent Motility, Phys. Rev. Lett. **108**, 248101 (2012).
[38] E. Bertin, H. Chaté, F. Ginelli, S. Mishra, A. Peshkov, and S. Ramaswamy, Mesoscopic theory for fluctuating active nematics, New J. Phys. **15**, 085032 (2013).
[39] B. Mahault, F. Ginelli, and H. Chaté (to be published).
[40] In 3D, we averaged over all directions of $\mathbf{q}_\perp$.
[41] A third intermediate scaling region with $\langle|\delta\rho(\mathbf{q})|^2\rangle \underset{q\to 0}{\sim} q_\parallel^{-2} q_\perp^{2-\zeta}$ is expected for $q_\perp^{\xi} \gg q_\parallel \gg q_\perp$ [27], but, given our estimate $\xi \simeq 1$ in both 2D and 3D, we expect it to be unobservable, at odds with the earlier results of Ref. [25].
[42] Note that our 2D results would be in disagreement with the TT theory under the hypothesis that the three scaling regimes observed would correspond to those predicted [see Eq. (6) and the intermediate one mentioned in Ref. [41]]. In particular, the third scaling regime we identify is independent of $q_\perp$.
[43] B. Delamotte, An introduction to the nonperturbative renormalization group, in *Renormalization Group and Effective Field Theory Approaches to Many-Body Systems*, edited by A. Schwenk and J. Polonyi (Springer, Berlin, 2012), pp. 49–132.